Solid State Communications 179 (2014) 20–24

Contents lists available at ScienceDirect

Solid State Communications

journal homepage: www.elsevier.com/locate/ssc

Magnetic properties and magnetocaloric effect in $SmNiC_2$ compound

Q.Y. Dong [a,*], L.C Wang [b], J. Chen [c], X.Q. Zhang [b], J.R. Sun [b], B.G. Shen [b]

[a] Department of Physics, Capital Normal University, Beijing 100048, People's Republic of China
[b] State Key Laboratory for Magnetism, Institute of Physics, Chinese Academy of Sciences, Beijing 100190, People's Republic of China
[c] Beijing Institute of Aerospace Testing Technology, China Aerospace Science and Technology Corporation, Beijing 100074, People's Republic of China

ARTICLE INFO

Article history:
Received 4 September 2013
Received in revised form
26 October 2013
Accepted 5 November 2013
by C. Lacroix
Available online 15 November 2013

Keywords:
C. $CeNiC_2$-type
D. First-order phase transition
D. Magnetic entropy change

ABSTRACT

Polycrystalline $SmNiC_2$ compound undergoes a first-order ferromagnetic transition around $T_C=17.5$ K and then an anomaly around $T_3=25.0$ K. The strong texture of polycrystalline $SmNiC_2$ sample as well as the application direction of magnetic field determines the magnitude of magnetization, further affecting the magnetic entropy change. Weak magneto-elastic coupling is responsible for the small shift of T_C with the increase of magnetic field, which leads to the invariability of the half maximum of the magnetic entropy change peak. Considering the strong magnetic anisotropy, a large magnetic entropy change ~14.1 J/kg K at 18 K for single crystal is estimated for a field change of 0–5 T along *a* axis. Large magnetocaloric effect and low cost indicate the potentiality of $SmNiC_2$ as a candidate for low-temperature magnetic refrigerant.

1. Introduction

In the bulk intermetallic materials, giant magnetocaloric effect (MCE) usually occurs at a magnetic field-induced magnetic phase transition such as from antiferromagnetic (or paramagnetic (PM)) to ferromagnetic (FM) state, which is simultaneously accompanied by a crystallographic transformation or considerable volume change. Typical examples of this class of materials are $Gd_5Si_{4-x}Ge_x$ [1,2], $La(Fe,M)_{13}$ (M=Si, Al, Co) [3], $MnFeP_xAs_{1-x}$ [4], RCo_2 (R=Ho, Er) [5–8], polycrystalline perovskite manganese oxides [9–11], shape memory alloys [12,13], etc. Magnetic refrigeration based on MCE is a promising technique due to its higher energy efficiency and friendly environment than the conventional gas compression refrigeration [14,15]. Currently, theoretical and experimental researches are still in progress for exploring new materials which have large MCE at low fields for the refrigeration technological application.

Recently, $RNiC_2$ (R=rare earth) compounds crystallized in the orthorhombic $CeNiC_2$-type structure (space group *Amm*2) have attracted much attention due to its various interesting physical properties such as magnetic ordering, superconductivity, meta-magnetism, charge-density wave (CDW) and so on [16–34]. Among these intermetallics, $SmNiC_2$ is unique in that it becomes ferromagnetic, while most of other members are prone to AFM instability. X-ray scattering experiments as well as electrical resistivity results of $SmNiC_2$ reveal satellite peaks corresponding to an incommensurate wave vector (0.5, 0.52, 0) below 148 K, signaling formation of a CDW state [28]. The abrupt disappearance of the satellite peak and the sharp decrease of the resistivity at the FM transition temperature ($T_C=17.4$ K) indicate a destruction of the CDW phase, and a strong correlation between the FM and CDW phases. First-principles electronic structure calculations [29] and the high-resolution photoemission spectroscopy study [30] find that Fermi-surface nesting is important for the CDW state and weaker nesting in the FM phase leads to the destruction of the CDW below T_C. The frustrated interchain coupling [31] and pseudogap state [30] imply the quasi-two-dimensional nature of the CDW in $SmNiC_2$. Moreover, the increase of pressure above 2.18 GPa can easily enhance the CDW transition temperature and lower the FM phase transition temperature and further change the FM phase transition nature to second order from first-order [32]. Besides the pressure, magnetic field can also affect the transition temperature of the CDW and FM states [33]. In addition, $SmNiC_2$ was also reported by Onodera et al. to exhibit anomalies at 13 K and 25 K in the magnetizations [25]. Multiple magnetic phase transition may lead to the quasi-platform of the MCE over the phase transition temperature range, which is very useful for Ericsson-cycle magnetic refrigerator [34]. So in the present paper, the magnetic properties and MCEs of $SmNiC_2$ are investigated by magnetization measurement. One peak and one cusp close to each other are observed on the curves of isothermal magnetic entropy change (ΔS) versus temperature due to the magnetic phase transitions. The maximal value of ΔS ~14.1 J/kg K at 18 K for single crystal is revealed for a field change of 0–5 T along *a* axis, suggesting that $SmNiC_2$ could be a promising candidate for magnetic refrigeration.

* Corresponding author. Tel.: +86 10 6890 7979.
E-mail address: happylaugh746@gmail.com (Q.Y. Dong).

0038-1098/$ - see front matter © 2013 Elsevier Ltd. All rights reserved.
http://dx.doi.org/10.1016/j.ssc.2013.11.012

2. Experiments

The $SmNiC_2$ compound was prepared by arc melting the constituent elements with the purity better than 99.9% in a high-purity argon atmosphere. Due to the vapor pressure of Sm, the initial stoichiometry of the compound was $Sm_{1.1}NiC_2$. The ingot was turned over and remelted four times to ensure its homogeneity. Then it was wrapped by a molybdenum foil, annealed in an evacuated sealed quartz tube at 1173 K for one week and quenched into liquid nitrogen. Powder X-ray diffractometer was performed to characterize the crystal structure of the samples. Magnetic measurements were carried out on a superconducting quantum interference device magnetometer. The three random pieces cut from the same ingot are named S0, Sa and Sb to carry out the magnetic measurements. The isothermal magnetization curves were measured from low temperature to high temperature in the heating process. Before measuring the next temperature, the magnetic field should be adjusted to 0 Oe to reduce the magnetic history effect. For sample S0, the magnetic field changes to 0 Oe when finishing the decreasing-field isothermal magnetization curve around T_C. For samples Sa and Sb, we just measure the increasing-field isothermal magnetization curves and after completing the measurement it is reduced to 0 Oe in an "oscillate" field mode. Obviously, the demagnetic result of the latter is greatly better than that of the former (see Fig. 4(a)–(c)).

3. Results and discussion

We prepare two powder samples from the same ingot to check the crystalline structure of $SmNiC_2$ compound. Fig. 1(a) and (b) shows the Rietveld refined powder X-ray diffraction patterns of $SmNiC_2$ compound at room temperature. They indicate that $SmNiC_2$ compound crystallize in an orthorhombic $CeNiC_2$-type structure except for the presence of very minor $SmO_{0.5}C_{0.4}$ phase marked at 30.4° and 35.2° and $SmNi_2$ phase marked at 41.2°. The structure refinements lead to rather good match between the experimental and calculated XRD patterns converging to acceptable Rietveld parameters Rp: 2.37 and 2.35 for two samples, respectively. The Sm atoms form two dimensional networks in the *a*-plane and the Ni and C atoms also form two dimensional networks in the ½ *a*-plane. These layers are laminated along the *a*-axis alternately (see the inset of Fig. 1(a)). The lattice parameters of both samples obtained from the refinement are the same. Their lattice parameters *a*, *b* and *c* equal to 3.706 Å, 4.529 Å and 6.098 Å, respectively, which almost accord with the previous report [25].

Fig. 2 displays the temperature (*T*) dependences of zero-field-cooling (ZFC) and field-cooling (FC) magnetizations (*M*) for S0 under a magnetic field of 0.1 T. Around $T_C = 17.5$ K, the magnetization changes abruptly and a small thermal hysteresis between ZFC and FC curves is observed, indicating the presence of the first-order phase transition (FOPT). The inset of Fig. 2 shows the ZFC and FC *M* vs. *T* curves around T_C under fields of 1 T and 5 T. It is worth mentioning that we choose additional small piece from the same ingot to carry out the measurement. One can find that the transition temperature is slightly shifted towards higher temperature with the increase of magnetic field. It is also one of the characters of FOPT. In addition, anomalies at ~25 K can be observed (see Fig. 2), as reported in Ref. [25] (where this temperature is defined as T_{t3}). However, any anomaly can not be found at ~13 K. In single-crystal $SmNiC_2$ compound, the inverse changes in the magnetizations along the *a* axis and along the *b* and *c* axes at this temperature, which is attributed to the population change of crystalline electric field levels [25], may lead to this disappearance of anomaly in the present compound.

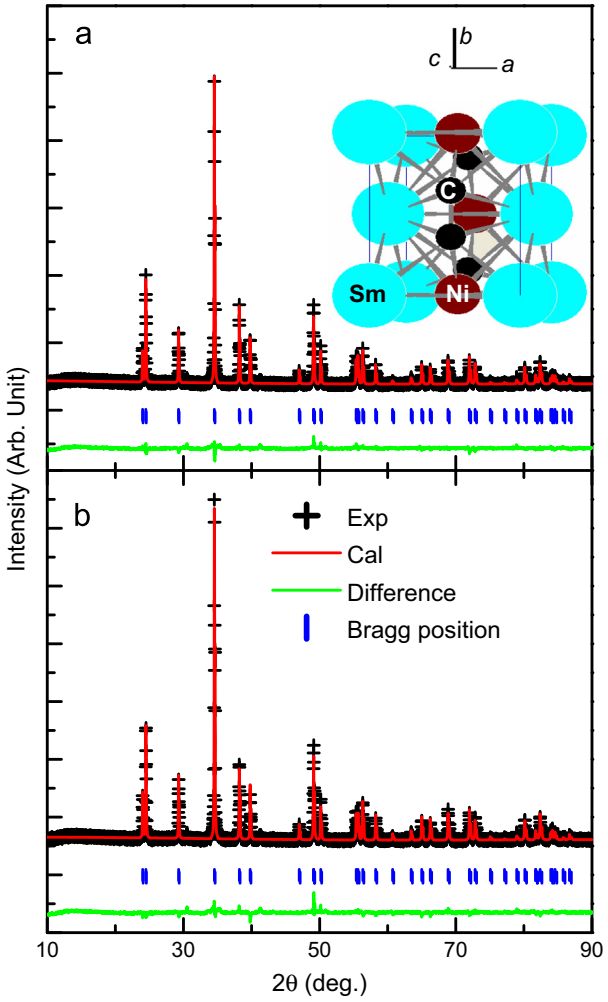

Fig. 1. (Color online) Rietveld refined powder XRD patterns (a) and (b) of two powder samples chosen randomly from the same $SmNiC_2$ ingot at room temperature, respectively. The observed data are indicated by crosses, and the calculated profile is the continuous line overlying them. The short vertical lines indicate the angular positions of the Bragg peaks of $SmNiC_2$. The lower curve shows the difference between the observed and calculated intensity. Inset of (a): schematic drawing of the $CeNiC_2$-type unit cell of $SmNiC_2$.

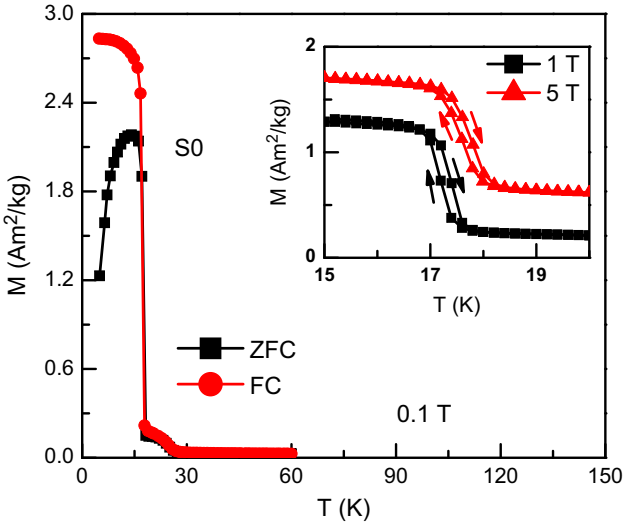

Fig. 2. (Color online) ZFC and FC temperature-dependent magnetization under a magnetic field of 0.1 T for S0. The inset shows the temperature variations of the ZFC and FC magnetization under 1 T and 5 T, respectively.

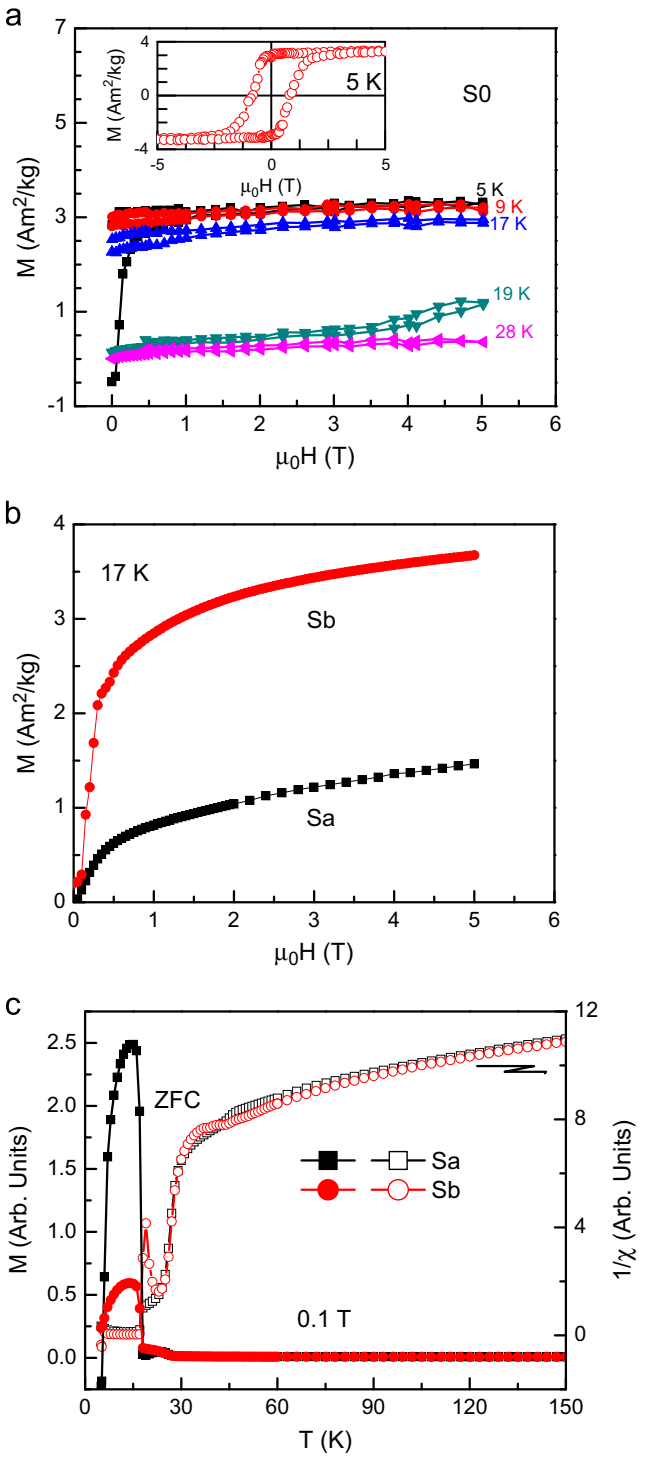

Fig. 3. (Color online) (a) Typical magnetic isothermals of $SmNiC_2$ measured during field increasing and decreasing, (b) initial magnetization curves at 17 K for two additional samples: Sa and Sb and (c) temperature dependences of ZFC magnetizations and the temperature variation of the ZFC inverse susceptibility under 0.1 T for Sa and Sb. The inset of (a) shows the hysteresis loop at 5 K.

The isothermal magnetization curves in the wide vicinity of Curie temperature during the field ascending and descending processes ranging from 0 to 5 T for S0 have been measured. For the sake of clarity, Fig. 3(a) displays the typical isothermal magnetization curves in the temperature range of 5–28 K. It is observed that each of M–H isotherms below T_C shows an irreversible behavior for the field increasing and decreasing cycles. Moreover, large remanence can also be found, which results in the large initial value of isothermal magnetization curves at the next measurement temperatures (See Fig. 3(a) in the present work and Fig. 2 in Ref. [33]) due to the effect of measuring mode as described in the experimental part. However, an obvious field-induced PM–FM metamagnetic transition with the hysteresis width of about 2 T occurs above T_C (for example, at 19 K, ~2 K above T_C), further indicating the nature of FOPT for $SmNiC_2$. The inset of Fig. 3(a) exhibits the magnetic hysteresis loop at 5 K. A coercive field of 0.83 T is observed, which is larger than that for single crystalline $SmNiC_2$ reported in Ref. [27]. The difference of microstructure between the present sample and the sample in Ref. [27] may lead to this phenomenon.

One can also see from Fig. 3(a) that the magnetization at 5 T and 5 K is 3.3 Am^2/kg, which is only about one third of that for single-crystalline $SmNiC_2$ with H along a axis in Ref. [25]. Similar phenomenon has been found in $CeNiC_2$ and $NdNiC_2$ [25]. In order to interpreting this divergence, we choose randomly two additional little pieces from the same ingot to measure the temperature and field dependences of magnetization. They were named as Sa and Sb. Fig. 3(b) depicts the isotherms at 17 K for two samples picked from a serial isothermal magnetization curves around T_C. Distinctly, their magnetization at 5 T is different from each other. Moreover, they are also lower than that value at 17 K in Fig. 3(a). Onodera et al. [25] reported that single-crystalline $SmNiC_2$ can be very easily magnetized to saturate along the a-axis by applying small magnetic field, whereas it shows very small magnetization along the b and c axes for the magnetic field up to 2 T at 5 K, suggesting the strong magnetic anisotropy of $SmNiC_2$.

Fig. 3(c) shows the temperature dependences of the ZFC magnetization and the reciprocal magnetic susceptibility χ^{-1} for Sa and Sb under the field of 0.1 T. The shape of M–T curves for S0, Sa and Sb is similar and these samples have the same phase transition temperature, confirming the homogeneity of the samples. However, the value of the magnetization is different from each other. Moreover, the reciprocal magnetic susceptibility of Sa and Sb still exists obvious discrepancy even up to 150 K. Combining with the results of isothermal magnetization, we think that the texture of polycrystalline sample as well as the application direction of magnetic field may lead to the discrepancy of magnetization for these samples.

Fig. 4(a)–(c) shows the isothermal magnetization curves of S0, Sa, and Sb around T_C during the field increasing process. At the same temperature and magnetic field, the value of magnetization is different. Moreover, the shape of M–H curve is also distinct especially around T_C. Based on the isothermal magnetization data, the isothermal magnetic entropy change can be calculated by Maxwell relation $\Delta S = \int_0^H (\partial M/\partial T)_H dH$. Sun et al. pointed out that this relation can be used to a system with a first-order phase transition if this system does not contain the coexistence of two phases in the vicinity of phase transition temperature [35,36]. The isothermal magnetization curves around T_C given by the present work and Refs. [25,33] indicate that the aforementioned condition is satisfied. So here using the Maxwell relation to evaluate the ΔS of $SmNiC_2$ is reasonable. Fig. 4(d)–(f) shows the temperature dependences of $-\Delta S$ for S0, Sa, and Sb for typical magnetic field changes. The magnetic entropy change for this compound is characterized by two anomalies: one spike-shaped peak centered at T_C and one cusp centered at T_{t3} (See the insets of Fig. 4(d)–(f)). The emergence of the peak around T_C is correlated with the FM–PM transition. Table 1 lists the magnetocaloric properties of S0, Sa, and Sb for the field changes of 0–2 T and 0–5 T. One can find that the peak height ($-\Delta S^{max}$) increases with increasing the magnetic field change ΔH. However, the half maximum of the peak (ΔT_{FWHM}) is not very sensitive to ΔH. This phenomenon is greatly different from those in the best known materials with a FOPT, such as MnAs [37], $LaFe_{13-x}Si_x$ [38], $Gd_5Si_2Ge_2$ [1], et al., where ΔT_{FWHM}

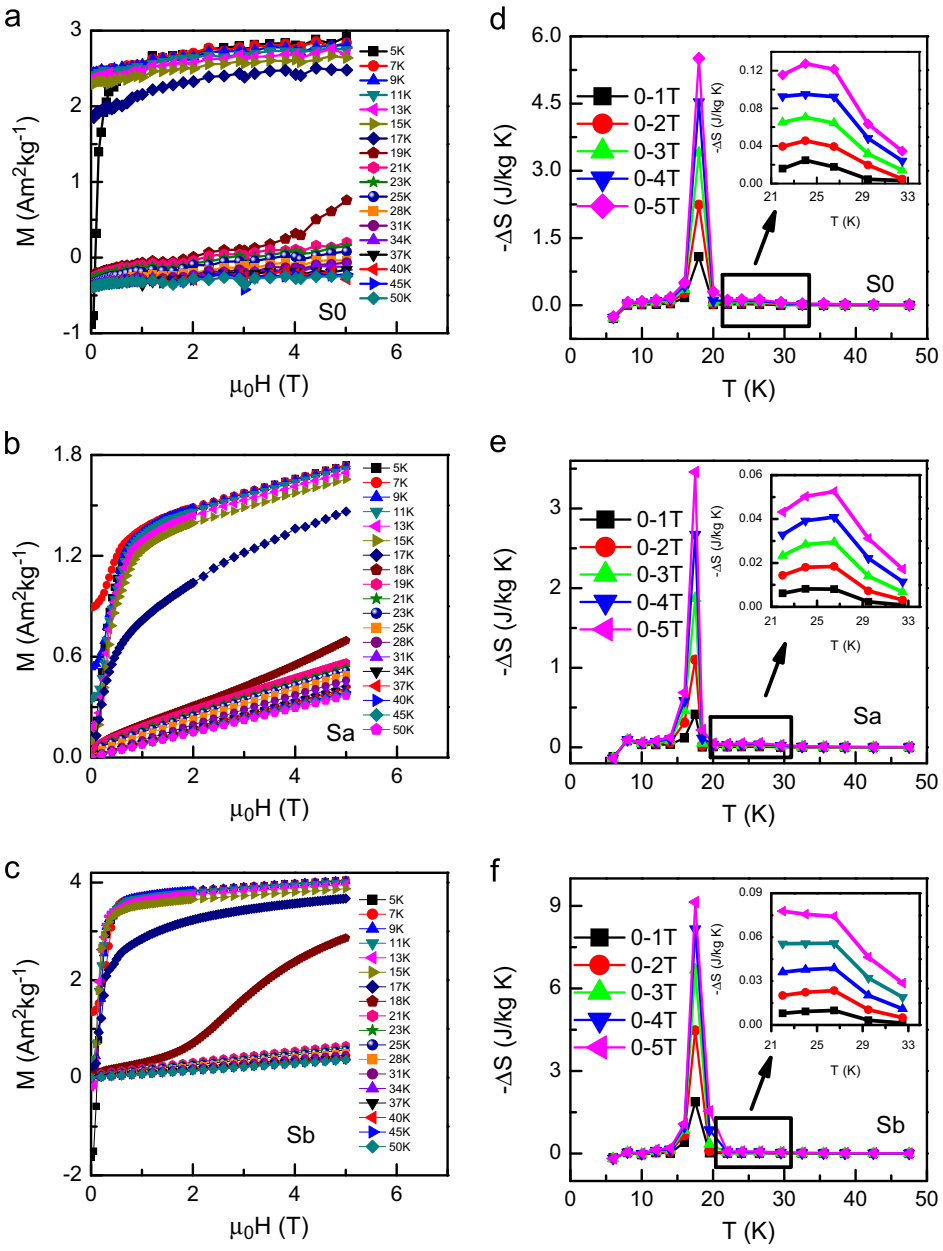

Fig. 4. (Color online) Magnetic isothermals (a)–(c) around T_C and temperature dependences of magnetic entropy change (d)–(f) in $SmNiC_2$ for different magnetic field changes for S0, Sa and Sb. The magnetic entropy change data around T_{t3} are shown in the insets of (d)–(f) for clarity.

Table 1
Magnetocaloric properties of $SmNiC_2$ samples S0, Sa and Sb for the field changes of 0–2 T and 0–5 T, respectively.

Sample ID	$-\Delta S^{max}$(0–2 T) (J/kg K)	$-\Delta S^{max}$(0–5 T) (J/kg K)	ΔT_{FWHM}(0–2 T) (K)	ΔT_{FWHM}(0–5 T) (K)
S0	2.2	5.5	2.0	2.1
Sa	1.1	3.5	1.5	1.5
Sb	4.5	9.1	1.9	2.0

increases with the increase of ΔH. The shift magnitude of the transition temperature driven by the magnetic field determines the value of ΔT_{FWHM}. One can find that the field change of 4 T induces T_C to shift toward higher temperature for only 0.4 K from the inset of Fig. 2. On the contrary, the phase temperature increases nearly linearly with an increase in magnetic field with a slope of 3.4 K/T in MnAs [37]. In $LaFe_{11.6}Si_{1.4}$, the phase temperature varies ~15 K with the magnetic field from 0.1 T to 4 T [39]. For $Gd_5Si_2Ge_2$ [1], the phase temperature is moved toward higher temperature for ~25 K when the magnetic field is increased to 5 T from 0 T. Therefore, $SmNiC_2$ is a very especial material with the FOPT. When $SmNiC_2$ undergoes the FM–PM phase transition, the $CeNiC_2$-type structure is always persisted [31]. It is reported in Ref. [26] that its lattice parameters *a*, *b* and *c* exhibit anomalous temperature dependence, from which we could deduce that the lattice volume change is small around T_C. It will lead to the weak magneto-elastic coupling and then the anomalous FOPT characters for $SmNiC_2$.

In addition, it can be clearly found from Fig. 4(d)–(f) that S0, Sa, and Sb exhibit different values of magnetic entropy change for the same field change. The strong texture of polycrystalline $SmNiC_2$ sample as well as the application direction of magnetic field determines the magnitude of magnetization, further affecting the magnetic entropy change. Considering the magnetization of single crystal with *H* along *a* axis reaches 9.3 Am^2/kg under the magnetic field of 5 T at 5 K [25], which is much higher than those of the

present samples, we could expect a larger value of ΔS. According to the M–H data at 17.5 K and 18.5 K for single crystal $SmNiC_2$ for fields applied along a axis in Ref. [33], the value of ΔS at 18 K is estimated to be 14.1 J/kg K for a field change of 0–5 T. This value is comparable with or much larger than those of the potential promising magnetic refrigerant materials in the similar temperature region under the same field change, such as $Dy_{0.9}Tm_{0.1}Ni_2B_2C$ (14.7 J/kg K) [40], DySb (15.8 J/kg K) [41], $PrCo_2B_2$ (8.1 J/kg K) [42], and $GdPd_2Si$ (15.0 J/kg K) [43].

4. Conclusion

The irreversibility of ZFC and FC magnetization curves around T_C as well as the metamagnetic transition above T_C indicates that polycrystalline $SmNiC_2$ undergoes a first-order ferromagnetic transition around T_C. Three samples from the same ingot with the alike phase transition temperature exhibit different value and shape for isothermal magnetization curves. The strong texture of polycrystalline $SmNiC_2$ sample as well as the application direction of magnetic field determines the magnitude of magnetization, further affecting the magnetic entropy change. The peak value of $-\Delta S$ increases with the increase of field changes, whereas the half maximum of the peak maintains constant due to the weak magneto-elastic coupling. Considering the strong magnetic anisotropy, the value of $-\Delta S$ at 18 K for single crystalline $SmNiC_2$ is estimated to reach 14.1 J/kg K for the same field change along a axis although its saturated magnetization is much lower than those of many typical magnetocaloric materials. The present study indicates that the first-order phase transition is very beneficial to obtain large magnetocaloric effect.

Acknowledgments

This work is supported by the National Natural Science Foundation of China (Grant nos. 51001077 and 11004204), the Hi-Tech Research and Development program of China, and the Beijing Excellent talent training support (Grant no. 2012D005016000002).

References

[1] V.K. Pecharsky, K.A. Gschneidner Jr., Phys. Rev. Lett. 78 (1997) 4494.
[2] V.K. Pecharsky, K.A. Gschneidner Jr., Appl. Phys. Lett. 70 (1997) 3299.
[3] F.X. Hu, B.G. Shen, J.R. Sun, Z.H. Chen, G.H. Rao, X.X. Zhang, Appl. Phys. Lett. 78 (2001) 3675.
[4] O. Tegus, E. Brück, K.H.J. Buschow, F.R. de Boer, Nature (London) 415 (2002) 150.
[5] N.A. de Oliveira, P.J. von Ranke, M.V. Tovar Costa, A. Troper, Phys. Rev. B 66 (2002) 094402.
[6] N.H. Duc, D.T. Kim Anh, P.E. Brommer, Physica B 319 (2002) 1.
[7] N.K. Singh, P. Kumar, K.G. Suresh, A.K. Nigam, A.A. Coelho, S. Gama, J. Phys.: Condens. Matter 19 (2007) 036213.
[8] H. Wada, Y. Tanabe, M. Shiga, H. Sugawara, H. Sato, J. Alloys Compd 316 (2001) 245.
[9] Z.B. Guo, Y.W. Du, J.S. Zhu, H. Huang, W.P. Ding, D. Feng, Phys. Rev. Lett. 78 (1997) 1142.
[10] P.G. Radaelli, D.E. Cox, M. Marezio, S.-W. Cheong, P.E. Schiffer, A.P. Ramirez, Phys. Rev. Lett. 75 (1995) 4488.
[11] X.X. Zhang, J. Tajada, Y. Xin, G.F. Sunm, K.W. Wong, X. Bohigas, Appl. Phys. Lett. 69 (1996) 3596.
[12] V. Recarte, J.I. Pérez-Landazabál, C. Gómez-Polo, E. Cesari, J. Dutkiewicz, Appl. Phys. Lett. 88 (2006) 132503.
[13] Y. Long, Z.Y. Zhang, D. Wen, G.H. Wu, R.C. Ye, Y.Q. Chang, F.R. Wan, J. Appl. Phys. 98 (2005) 046102.
[14] K.A. Gschneidner Jr., V.K. Pecharsky, A.O. Tsokol, Rep. Prog. Phys 68 (2005) 1479. (and references therein).
[15] A.M. Tishin, Y.I. Spichkin, in: J.M.D. Coey, D.R. Tilley, D.R. Vij (Eds.), The Magnetocaloric Effect and its Applications, Institute of Physics, London, 2003.
[16] J.K. Yakinthos, P.A. Kotsanidis, W. Schäfer, G. Will, J. Magn. Magn. Mater. 89 (1990) 299.
[17] J.K. Yakinthos, P.A. Kotsanidis, W. Schäfer, G. Will, J. Magn. Magn. Mater. 102 (1991) 71.
[18] J.K. Yakinthos, P.A. Kotsanidis, W. Schäfer, W. Kockelmann, G. Will, W. Reimers, J. Magn. Magn. Mater. 136 (1994) 327.
[19] H. Onodera, N. Uchida, M. Ohashi, H. Yamauchi, Y. Yamaguchi, N. Sato, J. Magn. Magn. Mater. 137 (1994) 35.
[20] H. Onodera, M. Ohashi, H. Amanai, S. Matsuo, H. Yamauchi, Y. Yamaguchi, S. Funahashi, Y. Mori, J. Magn. Magn. Mater. 149 (1995) 287.
[21] N. Uchida, H. Onodera, M. Ohashi, Y. Yamaguchi, N. Sato, S. Funahashi, J. Magn. Magn. Mater. 145 (1995) L16.
[22] S. Matsuo, H. Onodera, M. Kosaka, H. Kobayashi, M. Ohashi, H. Yamauchi, Y. Yamaguchi, J. Magn. Magn. Mater. 161 (1996) 255.
[23] W. Schäfer, W. Kochelmann, G. Will, J.K. Yakinthos, P.A. Kotsanidis, J. Alloys Compd. 250 (1997) 565.
[24] Y. Koshikawa, H. Onodera, M. Kosaka, H. Yamauchi, M. Ohashi, Y. Yamaguchi, J. Magn. Magn. Mater. 173 (1997) 72.
[25] H. Onodera, Y. Koshikawa, M. Kosaka, M. Ohashi, H. Yamauchi, Y. Yamaguchi, J. Magn. Magn. Mater. 182 (1998) 161.
[26] M. Murase, A. Tobo, H. Onodera, Y. Hirano, T. Hosaka, S. Shimomura, N. Wakabayashi, J. Phys, Soc. Jpn. 73 (2004) 2790.
[27] M. Mizumaki, N. Kawamura, H. Onodera, Phys. Stat. Sol. (c) 3 (2006) 2767.
[28] S. Shimomura, C. Hayashi, G. Asaka, N. Wakabayashi, M. Mizumaki, H. Onodera, Phys. Rev. Lett. 102 (2009) 076404.
[29] J. Laverock, T.D. Haynes, C. Utfeld, S.B. Dugdale, Phys. Rev. B 80 (2009) 125111.
[30] T. Sato, S. Souma, K. Nakayama, T. Takahashi, S. Shimomura, H. Onodera, J. Phys. Soc. Jpn. 79 (2010) 044707.
[31] A Wölfel, L. Li, S. Shimomura, H. Onodera, S. Van Smaalen, Phys. Rev. B 82 (2010) 054120.
[32] B. Woo, S. Seo, E. Park, J.H. Kim, D. Jang, T. Park, H. Lee, F. Ronning, J. D. Thompson, V.A. Sidorov, Y.S. Kwon, Phys. Rev. B 87 (2013) 125121.
[33] N. Hanasaki, Y. Nogami, M. Kakinuma, S. Shimomura, M. Kosaka, H. Onodera, Phys. Rev. B 85 (2012) 092402.
[34] H. Takeya, V.K. Pecharsky, K.A. Gschneidner Jr., J.O. Moorman, Appl. Phys. Lett. 64 (1994) 2739.
[35] J.R. Sun, F.X. Hu, B.G. Shen, Phys. Rev. Lett. 85 (2000) 4191.
[36] G.J. Liu, J.R. Sun, J. Shen, B. Gao, H.W. Zhang, F.X. Hu, B.G. Shen, Appl. Phys. Lett. 90 (2007) 032507.
[37] H. Wada, Y. Tanabe, Appl. Phys. Lett. 79 (2001) 3302.
[38] F.X. Hu, Max llyn, A.M. Tishin, J.R. Sun, G.J. Wang, Y.F. Chen, F. Wang, Z. H. Cheng, B.G. Shen, J. Appl. Phys. 93 (2003) 5503.
[39] Q.Y. Dong, H.W. Zhang, J. Shen, J. Chen, J.R. Sun, B.G. Shen, J. Appl. Phys. 111 (2012) 07E107.
[40] L.W. Li, K. Nishimura, Appl. Phys. Lett. 95 (2009) 132505.
[41] W.J. Hu, J. Du, B. Li, Q. Zheng, Z.D. Zhang, Appl. Phys. Lett. 92 (2008) 192505.
[42] L.W. Li, K. Nishimura, J. Appl. Phys. 106 (2009) 023903.
[43] R. Rawat, I. Das, J. Phys.: Condens. Matter 13 (2001) L57.